

Thermodynamics of Ultracold Fermions in Traps

Qijin Chen,* Jelena Stajic, and K. Levin

James Franck Institute and Department of Physics, University of Chicago,
5640 South Ellis Avenue, Chicago, Illinois 60637, USA

*To whom correspondence should be addressed; E-mail: qchen@uchicago.edu.

The ability to tune the strength of the attractive interaction in trapped Fermi gases is revealing the nature of superfluidity (and superconductivity) in a hitherto unexplored regime. Within the last few years we have witnessed the discovery of strongly interacting Fermi gases; over the last year we have found strong evidence for their superfluidity. These interacting gases appear at intermediate coupling and are the most complex. We do not know the nature of the fermionic and bosonic excitations and, until recently (1), measurements of temperature have been problematic, largely because of the absence of theoretical guidance. This paper probes these fundamental questions through studies of thermodynamics, leading to good quantitative agreement with experiment (1).

cond-mat/0411090

It is now widely believed that superfluidity has been observed (2, 3, 4, 5) in trapped atomic gases containing fermionic atoms at micro-Kelvin temperatures. This superfluidity is closely connected to superconductivity, which is a very common state of metals at low temperatures, of the order of tens of Kelvin. Of great interest is the fact that this superfluidity may also connect to the less well understood phenomenon of high temperature superconductivity (6).

Our understanding of conventional superconductors is based on a remarkable theory called the Bardeen-Cooper-Schrieffer (BCS) theory. However, the atomic gases have a new capability, not found in metallic superconductors. Via magnetic fields, one can tune the strength of the attractive interaction by coupling to a Feshbach resonance (7, 8, 9). This attractive interaction is what causes fermions to pair up into bosonic-like states (Cooper pairs). Ultimately these bosons are driven by their statistics to condense at temperature T_c . BCS theory is based on a simple ground state wavefunction, in the presence of very weak attraction. Importantly, some years ago (10) it was shown that this same wavefunction (or mean field ground state) can be contemplated for arbitrary attraction, thereby effecting a crossover from BCS theory to Bose Einstein condensation (BEC).

The theoretical community is in the midst of unraveling the nature of these fermionic superfluids (11, 12, 13, 14, 15, 16, 17, 18, 19) with particular emphasis on the strongly interacting Fermi gas (20). Indeed, one might argue that the well studied BCS and BEC limits are special cases and that the more robust limit of superfluidity corresponds to this intermediate coupling case. Via collective mode (17, 16) and radio frequency (RF) spectroscopy studies (15), reasonably strong theoretical support has been found for the BCS-like wavefunction (10) which describes this crossover, at least semi-quantitatively. What precisely is the nature of the excitations from this ground state is the topic of the present paper. In the process of addressing this issue we are able, (in conjunction with recent experiments (1)), to help provide a theoretical calibration of the experimental thermometry, and elucidate the thermodynamics.

Unlike the situation in condensed matter systems, for these ultracold gases direct thermometry is less straightforward. Experimentally, “temperature” is conventionally measured in the ($T > T_c$) BCS or weak attraction regime, by fitting density or atomic momentum distribution profiles to that of a non-interacting Fermi gas (2, 3). In the opposite BEC regime, temperature can be deduced by fitting the Gaussian wings of density profiles (21). Thus, it is convenient

to describe a given intermediate regime which is accessed adiabatically, by giving the initial temperature at either endpoint. In order to determine this adiabatically accessed temperature, one needs precise knowledge of the entropy S as a function of T from BCS to BEC.

Without doing any calculations one can anticipate a number of features of thermodynamics in the crossover scenario. The excitations are entirely bosonic in the BEC regime, exclusively fermionic in the BCS regime, and in between both types of excitation are present. In the so-called one-channel problem the “bosons” correspond to noncondensed Cooper pairs, whereas in two-channel models, these Cooper pairs are strongly hybridized with the molecular bosons of the closed channel, singlet state. Below T_c the presence of the condensate leads to a single-branch bosonic excitation spectrum, which, at intermediate coupling is predominantly composed of large Cooper pairs. These latter bosons, as “preformed pairs”, are also present above T_c , and are associated with a fermionic excitation gap (or pseudogap (6, 22)). This is to be distinguished from the “gap” of BCS theory, which vanishes at T_c .

The unitary regime, where the inter-atomic s -wave scattering length a diverges, is the most interesting to the community (20). Importantly, in the ultracold fermion gases near unitarity, experimental evidence for a pseudogap, consistent with these preformed pairs, has been reported recently (23, 24). Within the conventional mean field ground state, and over the entire crossover regime (25) below T_c , the bosons have dispersion $\Omega_q = \hbar^2 q^2 / 2M^*$. This form for the dispersion reflects the absence of direct boson-boson interactions. Rather the bosons are presumed to interact only via the fermions. This ground state is, thus, limited to a regime where the fermions are still in evidence. The reasonably good semi-quantitative agreement between experimental (4, 5, 26) and theoretical (17, 16) collective mode studies suggests that there exists a near-BEC regime, where the mean field ground state wavefunction is adequate. At some stage, when the fermionic degrees of freedom become irrelevant, direct inter-boson interactions must be accounted for and they will alter the collective mode behavior (18). While, our focus

in this paper is on the unitary case, when we refer to “BEC” we restrict our attention to this experimentally accessible (4, 5) (or near-BEC) regime.

As long as the attractive interactions are stronger than those of the BCS regime, these non-condensed pairs must show up in thermodynamics, as must the pseudogap in the fermionic spectrum. These are two sides of the same coin. In the absence of a trap, and quite generally, for $T < T^*$, where T^* is defined as the pseudogap onset temperature with $T^* > T_c$, there is a finite gap Δ for fermionic excitations. At and below T_c these fermions have dispersion $E_{\mathbf{k}} = \sqrt{(\epsilon_{\mathbf{k}} - \mu)^2 + \Delta^2}$, where $\epsilon_{\mathbf{k}} = \hbar^2 k^2 / 2m$ and μ are the atomic kinetic energy and fermionic chemical potential, respectively. That this gap is non-zero at T_c in the Bogoliubov quasi-particle spectrum $E_{\mathbf{k}}$, differentiates the present approach (25) from all other schemes which address BCS-BEC crossover at finite T . The bosons, by contrast, are gapless in the superfluid phase, due to their vanishing chemical potential. Within a trap, and in the fermionic regime (for which $\mu > 0$), the fermionic component will have a strong spatial inhomogeneity via the spatial variation of the gap. Thus, in contrast to the homogeneous case, fermions on the edge of the trap, which have relatively small or vanishing excitation gaps Δ , will contribute power law dependences to the thermodynamics. These same edge effects have been invoked in analyzing recent RF experiments (23, 15).

It is relatively straightforward to compute the thermodynamical properties of the BCS-BEC crossover system within a consistent many-body theory (27, 28) based on the conventional mean field state. Our formalism was also applied to explain earlier RF experiments by Kinnunen *et al* (15). We note that although a one-channel model is a good approximation in the unitary regime and for broad resonances, one needs the two-channel model (22) discussed here, in order to accurately describe the BEC regime. As expected there are two contributions to the entropy (and energy E) arising from fermionic, S_f and bosonic, S_b excitations. To address the thermodynamics in the trap, we need to integrate S and E over the trap, where we use

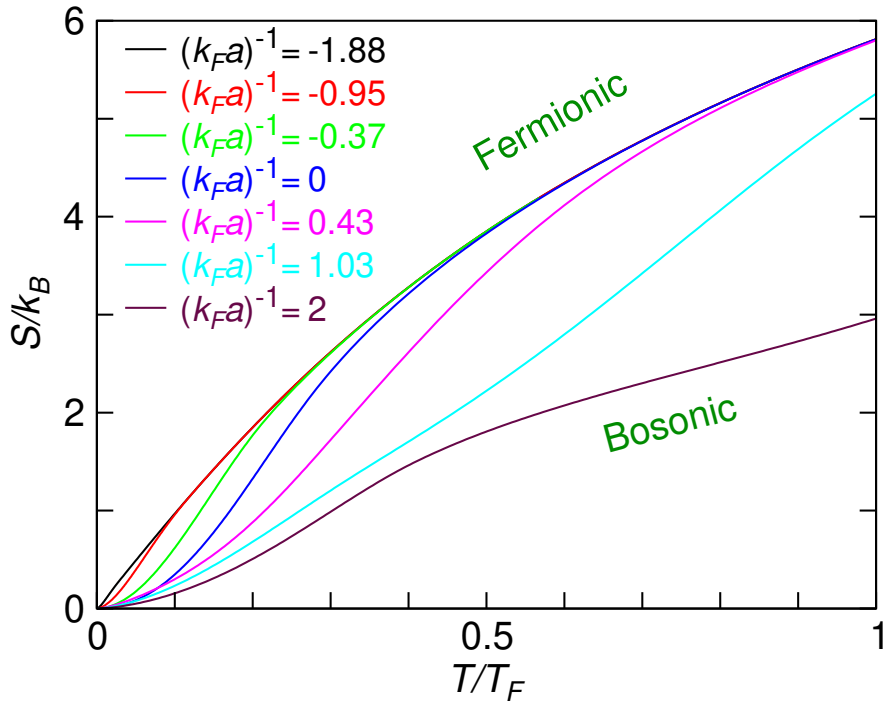


Figure 1: Entropy per atom as function of temperature for different values of the dimensionless parameter $(k_Fa)^{-1}$. Here a is the inter-atomic s -wave scattering length, k_F is the Fermi wave vector, and T_F is the noninteracting Fermi temperature at the trap center. The curves $(k_Fa)^{-1} = -1.88, 0$, and 2 correspond to the BCS, unitary, and BEC cases, respectively.

previously calculated (29) profiles of the various gaps and the particle density as a function of the radius.

Figure 1 illustrates the behavior of S over the entire crossover regime. The magnetic field is contained in the dimensionless parameter $(k_Fa)^{-1}$, which increases with field. Here k_F is the Fermi wave vector. As can be seen in the figure, the fermionic power laws are particularly evident in the high field or BCS regime ($(k_Fa)^{-1} = -1.88$), where the edge fermions behave like a normal Fermi gas and lead to a linear T dependence in S_f over a wide range of temperatures. As T is further raised, the entropy exhibits a slower than linear T dependence, as the chemical potential drops to 0; here the system is no longer a degenerate Fermi gas. For high fields, the bosonic degrees of freedom are essentially irrelevant.

By decreasing the magnetic field, we tune from the BCS-like regime towards unitarity. We first consider low T where fermions become paired over much of the trap. Those unpaired fermions which are present are at the edge. They tend to dominate the thermodynamics associated with the fermionic degrees of freedom, and, importantly in a trap, lead to a higher powers (than linear) in their T dependence. The contribution from excited pairs of fermions (Cooper pairs at finite momentum) is associated with a $T^{3/2}$ dependence of entropy on temperature which dominates for temperatures $T/T_F \lesssim 0.05$ or $T/T_c \lesssim 0.2$. In general, the overall exponent of the low T power law varies with magnetic field, depending on the magnitude of the gap and temperature, as well as the relative weight of fermionic and bosonic contributions. In the superfluid phase, at all but the lowest temperatures, the fermions and bosons combine to yield $S \propto T^2$ precisely at resonance ($(k_F a)^{-1} = 0$). We will focus on a “near unitary” case here ($(k_F a)^{-1} = 0.11$), for which $S \propto T^{1.9}$. This corresponds to being slightly below the resonance, by about 1% of the resonance width.

At the other extreme, at sufficiently high $T \approx T^*$, the entropy approaches that of the non-interacting system. It is appropriate to think of this temperature as the “pseudogap onset” temperature; it lies significantly above T_c for the unitary case shown here ($T_c/T_F = 0.27$, $T^* \approx 0.5T_F$). This temperature should be associated with the opening of a normal state excitation gap which reflects the formation of meta-stable pair states. Interestingly, in the unitary regime, T^* is not far away from the break-down of Fermi degeneracy, which occurs when $\mu \approx 0$ or $T/T_F \approx 0.6$.

As the field decreases further below the resonance, T^* rapidly increases and the system ultimately enters the near-BEC regime. Here we see a pure $T^{3/2}$ power law in S at low T , associated with the quadratic (q^2) bosonic dispersion relation. This is to be contrasted with the T^3 dependence found by Williams and co-workers (14) who considered non-interacting, but trapped, fermions and bosons. Similarly a T^3 dependence is found for true bosons in a

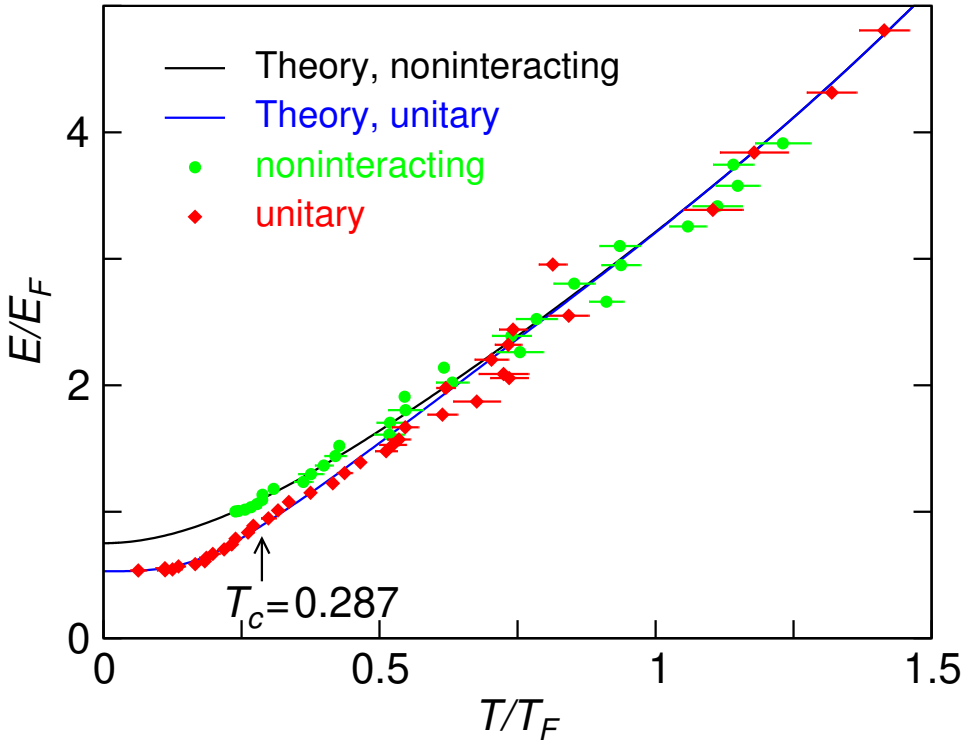


Figure 2: Comparison of present theory (lines) and experiments (symbols) of Ref. (1) in terms of E/E_F as a function of T/T_F , for both unitary ($(k_F a)^{-1} = 0.11$) and noninteracting cases, with Gaussian trap potential having trap depth $V_0/E_F = 14.6$ as in experiment. The fact that the two experimental (and the two theoretical) curves begin to separate below $T^* > T_c$ is consistent with the presence of a pseudogap.

trap, in the presence of boson-boson interactions (13). To establish the $T^{3/2}$ power law found here it is important to note that there is no direct boson-boson coupling, and that fermion-boson interactions are responsible for the vanishing of μ_{pair} in the superfluid regions. The latter implies that, within a trap, the associated power laws in the entropy are the same as those of the homogeneous system, as found elsewhere in a related context (13). Clearly, the groundstate ansatz will be inapplicable at some point when the fermionic degrees of freedom have completely disappeared, and the gas is deep in the BEC regime.

We test these consequences of the mean field ground state in Fig. 2 which shows a comparison of the associated energy versus temperature for the non-interacting and unitary regimes,

as compared to recent experimental data (1). To make contact with experiment (1) here we consider a realistic Gaussian trap potential, $V(r) = V_0[1 - e^{-m\omega^2 r^2/2V_0}]$. The broad Feshbach resonances in both ^{40}K and ^6Li allow us to tune the magnetic field [$(k_F a)^{-1} = 0.11$], slightly away from resonance so that the unitary gas parameter β ($= -0.49$) (20, 11), has the same value as in experiment. Consistent with Ref. (1), the experimental unitary data were first converted to the units of noninteracting Fermi energy $E_F = k_B T_F$ by a simple rescaling of both energy and temperature by $\sqrt{1 + \beta}$. This figure shows that both the unitary and non-interacting cases coincide above T^* , although below T_c they start out with different power laws. In the figure the experimental temperature data is recalibrated. Such a recalibration only affects the temperature scales for $T \leq T_c$. The recalibration was performed by applying the same experimental fitting procedure (28) to the theoretically obtained density profiles (29). Agreement between theory and experiment is very good over the full temperature range shown. The observation that the interacting and non-interacting curves do not coincide until temperatures significantly above T_c is consistent with (although it does not prove) the existence of a pseudogap with onset temperature from the figure $T^* \approx 2T_c$. Very similar effects are seen in the thermodynamics of high temperature superconductors (6). Note that the superfluid transition will manifest itself as a change in power law exponent across T_c when Fig. 2 is plotted on a log-log scale, as shown in Fig. S4 (28).

Finally, Fig. 3 presents a blow-up of the low temperature regime of the previous figure. Although the theoretical calculations are for a spherical, not highly asymmetric trap (30), the agreement between theory and experiment is very good. This figure reflects the fact that the thermodynamics at low T is governed by a combination of two contributions: from the fermions at the edge of the trap and from the pair excitations of the condensate.

In this paper we have laid the groundwork for characterizing the “bosonic” and fermionic excitations and for measuring temperature in the strongly interacting Fermi gas; we have done

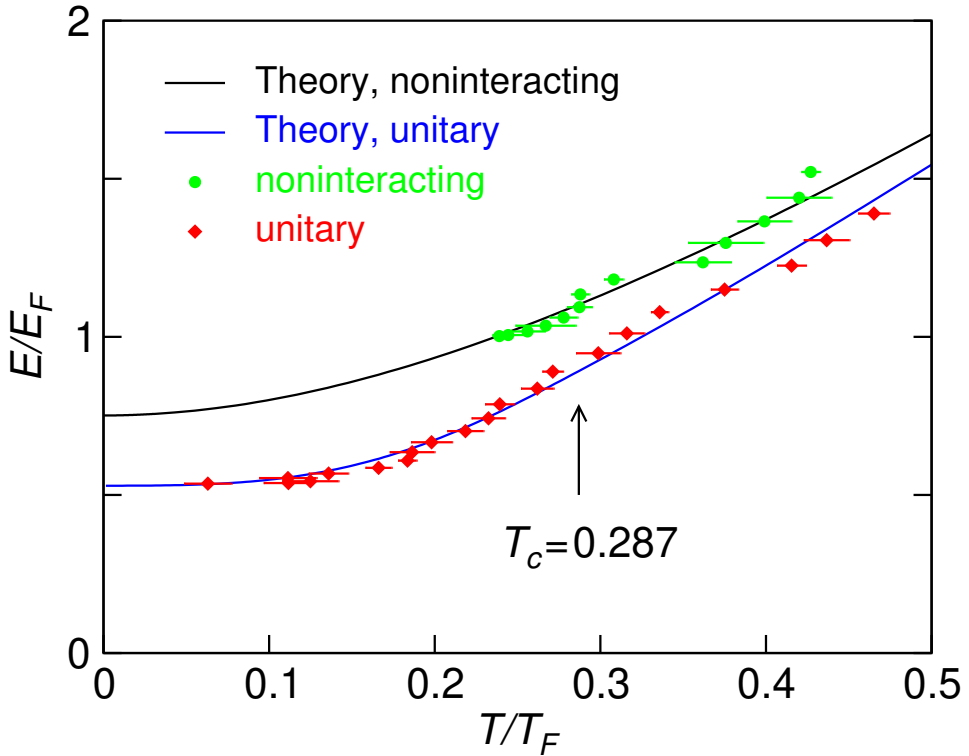


Figure 3: Low temperature comparison of present theory and experiments of Ref. (1) in terms of E/E_F as a function of T/T_F , for both unitary and noninteracting cases, with Gaussian trap potential, as in Fig. 2.

this by addressing both thermodynamical and density profile data (1). These experimental and theoretical studies represent a necessary first step, beyond the initial discovery stage, in arriving at an understanding of the fermionic superfluids. The good agreement with experiment suggests that the present theory based on the widely studied (6, 25, 15, 17, 16) mean field ground state provides a quantitatively reasonable description of the thermodynamics of strongly interacting Fermi gases in traps.

References and Notes

1. J. Kinast, A. Turlapov, J. E. Thomas, Heat capacity of a strongly interacting fermi gas. Preprint available at <http://arXiv.org/abs/cond-mat/0409283>.
2. C. A. Regal, M. Greiner, D. S. Jin, *Phys. Rev. Lett.* **92**, 040403 (2004).
3. M. W. Zwierlein, *et al.*, *Phys. Rev. Lett.* **92**, 120403 (2004).
4. J. Kinast, *et al.*, *Phys. Rev. Lett.* **92**, 150402 (2004).
5. M. Bartenstein, *et al.*, *Phys. Rev. Lett.* **92**, 203201 (2004).
6. Q. J. Chen, J. Stajic, S. N. Tan, K. Levin, BCS-BEC crossover: From high temperature superconductors to ultracold superfluids. Preprint available at <http://arXiv.org/abs/cond-mat/0404274>.
7. M. Holland, S. J. J. M. F. Kokkelmans, M. L. Chiofalo, R. Walser, *Phys. Rev. Lett.* **87**, 120406 (2001).
8. E. Timmermans, K. Furuya, P. W. Milonni, A. K. Kerman, *Phys. Lett. A* **285**, 228 (2001).
9. Y. Ohashi, A. Griffin, *Phys. Rev. Lett.* **89**, 130402 (2002).
10. A. J. Leggett, *Modern Trends in the Theory of Condensed Matter* (Springer-Verlag, Berlin, 1980), pp. 13–27.
11. T.-L. Ho, *Phys. Rev. Lett.* **92**, 090402 (2004).
12. A. Perali, P. Pieri, L. Pisani, G. C. Strinati, *Phys. Rev. Lett.* **92**, 220404 (2004).
13. L. D. Carr, G. V. Shlyapnikov, Y. Castin, *Phys. Rev. Lett.* **92**, 150404 (2004).

14. J. E. Williams, N. Nygaard, C. W. Clark, Phase diagrams for an ideal gas mixture of fermionic atoms and bosonic molecules. Preprint available at <http://arXiv.org/abs/cond-mat/0406617>.
15. J. Kinnunen, M. Rodriguez, P. Törmä, *Science* **305**, 1131 (2004).
16. H. Heiselberg, *Phys. Rev. Lett.* **93**, 040402 (2004).
17. H. Hu, A. Minguzzi, X.-J. Liu, M. P. Tosi, Collective modes and ballistic expansion of a Fermi gas in the BCS-BEC crossover. Preprint available at <http://arXiv.org/abs/cond-mat/0404012>.
18. S. Stringari, *Europhys. Lett.* **65**, 749 (2004).
19. C. Chin, A simple mean field equation for condensates in the BEC-BCS crossover regime. Preprint available at <http://arXiv.org/abs/cond-mat/0409489>.
20. K. M. O'Hara, *et al.*, *Science* **289**, 2179 (2002).
21. M. Bartenstein, *et al.*, *Phys. Rev. Lett.* **92**, 120401 (2004).
22. J. Stajic, Q. J. Chen, K. Levin, Particle density distributions in fermi gas superfluids: Differences between one and two channel models in the BEC limit. Preprint available at <http://arXiv.org/abs/cond-mat/0402383>.
23. C. Chin, *et al.*, *Science* **305**, 1128 (2004).
24. M. Greiner, C. A. Regal, D. S. Jin, Probing the excitation spectrum of a Fermi gas in the BCS-BEC crossover regime. Preprint available at <http://arXiv.org/abs/cond-mat/0407381>.
25. J. Stajic, *et al.*, *Phys. Rev. A* **69**, 063610 (2004).

26. J. Kinast, A. Turlapov, J. E. Thomas, Breakdown of hydrodynamics in the radial breathing mode of a strongly-interacting fermi gas. Preprint available at <http://arXiv.org/abs/cond-mat/0408634>.
27. Q. J. Chen, K. Levin, I. Kosztin, *Phys. Rev. B* **63**, 184519 (2001).
28. Materials and methods are available as supporting material on *Science* Online.
29. J. Stajic, Q. J. Chen, K. Levin, Measuring condensates in fermionic superfluids via density profiles in traps. Preprint available at <http://arXiv.org/abs/cond-mat/0408104>.
30. It can be shown that trap anisotropy is not relevant for thermodynamical quantities because they involve integrals over the entire trap. The calculations can be mapped onto an equivalent isotropic system.
31. We are extremely grateful to J.E. Thomas, J. Kinast and A. Turlapov for many helpful discussions, and for sharing their data before publication. Useful conversations with N. Nygaard and Cheng Chin are also acknowledged. This work was supported by NSF-MRSEC Grant No. DMR-0213745 and in part by the Institute for Theoretical Sciences, ND-ANL (QC).

Supporting Online Material

www.sciencemag.org

Materials and Methods

Figs. S1, S2, S3, S4

References and Notes

Supporting Online Material

Our calculations are based on the standard mean field ground state (1). In this way we differ from other work (2, 3) at finite temperatures. Elsewhere (4, 5, 6) we have characterized in quantitative detail the characteristic gap Δ , and pseudogap, Δ_{pg} energy scales. The pseudogap (which is to be associated with a hybridized mix of noncondensed fermion pairs and molecular bosons) and the superfluid condensate (sc) called $\tilde{\Delta}_{sc}$, add in quadrature to determine the fermionic excitation spectrum: $\Delta^2(T) = \tilde{\Delta}_{sc}^2(T) + \Delta_{pg}^2(T)$. Our past work (4, 5, 6) has primarily focussed below T_c . Here we extend these results, albeit approximately, above T_c . Our formalism has been applied below T_c with some success by Kinnunen *et al* (7) to measurements of the pairing gap in RF spectroscopy. A more precise, but numerically less accessible method for addressing the normal state was given in Ref. (8).

For generality, we consider the two channel Hamiltonian in which there are both molecular or Feshbach bosons (FB) and finite momentum Cooper pairs, as well as fermionic quasi-particles. The condensate, like the bosonic excitations, should be viewed as a strongly hybridized mixture of Cooper pairs and FB. In this two channel picture the effective interaction includes pairing in the open channel (via U) and through the Feshbach resonance (via g), so that the effective pairing strength (9, 10) is given by $U_{eff}(Q) = U + g^2 D_0(Q) \equiv U + \frac{g^2}{i\Omega_n - E_q^b + 2\mu - \nu}$, where $U_{eff}(0) \equiv U + \frac{g^2}{2\mu - \nu}$. Here $Q \equiv (i\Omega_n, \mathbf{q})$ is a 4-momentum, $\Omega_n = 2n\pi T$ ($n = \text{integer}$) is the bosonic Matsubara frequency, and $E_q^b = q^2/4m$ represents the molecular boson dispersion.

Our self consistent equations, which have been presented elsewhere in some detail (4), can be approximately extended above T_c by including a self consistently determined non-vanishing pair chemical potential, μ_{pair} (and its molecular bosonic counterpart, μ_{boson}). These self consistent equations determine the unknowns: $\Delta(T)$, $\Delta_{pg}(T)$, the bosonic dispersion $\Omega_{\mathbf{q}}$, as well as μ , μ_{pair} and μ_{boson} . For notational simplicity, we omit writing the trap potential $V(r)$ which

is to be added everywhere that the fermionic chemical potential appears according to the LDA prescription: $\mu \rightarrow \mu - V(r)$.

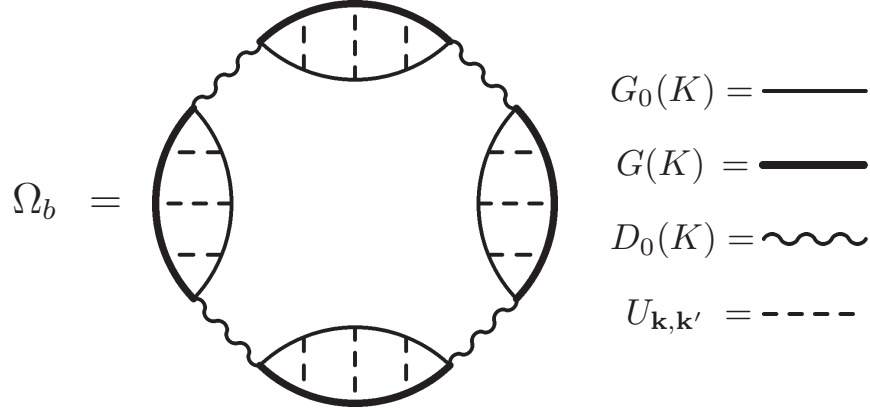


Figure S1: Bosonic contribution to the thermodynamical potential. Here G_0 (G) and D_0 (D) are the “bare” (“full”) propagators associated with the fermions and molecular Feshbach bosons, respectively, and $U_{\mathbf{k},\mathbf{k}'}$ is the open-channel pairing interaction.

Our first equation represents the important defining condition for the pair chemical potential: that the inverse pair propagator or T-matrix $t(Q)$ at $Q \equiv 0$ is proportional to μ_{pair} , with coefficient of proportionality given by a (inverse) “residue” Z . (The various residues Z and Z_b which appear below can be readily computed (11, 12), but are of no particular interest here). Importantly, in the superfluid regions of the trap $\mu_{pair} = \mu_{boson} \equiv 0$. We have

$$U_{eff}^{-1}(0) + \sum_{\mathbf{k}} \frac{1 - 2f(E_{\mathbf{k}})}{2E_{\mathbf{k}}} = Z\mu_{pair}, \quad (1)$$

where $f(x)$ is the Fermi distribution function. The pseudogap contribution can be written in terms of the usual Bose distribution function $b(x)$ by

$$\Delta_{pg}^2 = \frac{1}{Z} \sum_{\mathbf{q}} b(\Omega_{\mathbf{q}} - \mu_{pair}). \quad (2)$$

The total atomic number N is given by integrating the local density of particles, $n(r)$, which

can be written

$$\begin{aligned}
n &= 2n_b^0 + \frac{2}{Z_b} \sum_{\mathbf{q}} b(\Omega_q - \mu_{boson}) \\
&\quad + 2 \sum_{\mathbf{k}} [v_{\mathbf{k}}^2(1 - f(E_{\mathbf{k}})) + u_{\mathbf{k}}^2 f(E_{\mathbf{k}})] .
\end{aligned} \tag{3}$$

where $n_b^0 = g^2 \Delta_{sc}^2 / [(\nu - 2\mu + 2V(r))U]^2$ is the molecular Bose condensate and $u_{\mathbf{k}}^2, v_{\mathbf{k}}^2$ are the usual coherence factors which appear in BCS theory. This FB condensate term enters, in conjunction with the open channel Cooper contribution (Δ_{sc}), to define the total order parameter (9, 10, 4): $\tilde{\Delta}_{sc} = \Delta_{sc} + |g| \sqrt{n_b^0}$. For simplicity, throughout we introduce units $k_B = 1$, $\hbar = 1$, fermion mass $m = \frac{1}{2}$, Fermi momentum $k_F = 1$, and noninteracting Fermi energy $E_F = \hbar\omega(3N)^{1/3} = 1$ for a harmonic trap $V(r) = m\omega^2 r^2/2$, where ω is the trap frequency (13).

To obtain the entropy S , we may start directly from the energy at a given T , which can be obtained from the underlying Green's functions of the theory. It is more intuitive, however, to begin with the corresponding thermodynamic potential, which helps to clarify the diagrammatic scheme, and to relate it to the simpler model of Ref. (14). This potential contains fermionic contributions from bare fermions, Ω_f , and bosonic contributions Ω_b . The latter is, to a good approximation (15), given by the sum of all possible ring diagrams shown in Fig. S1. Each diagram contains at least one bare boson line or one fermion pair bubble, associated with the open channel. As in previous work (4), our bubble diagrams involve one dressed and one bare Green's function. One can demonstrate self consistency between our self energy diagrams (4) and this thermodynamical potential by cutting different lines in the diagram of Figure S1. When we cut a boson line, we obtain the non-interacting boson propagator and all self-energy diagrams of bosons, which sum to give the fully dressed boson propagator $D(Q)$. When cutting a fermion line, we will end up with the fermion self-energy diagrams, which when combined with the bare fermion propagator $G_0(K)$ derived from Ω_f will give the fully dressed fermion propagator, $G(K)$.

After regrouping, we see that the energy and the entropy have two contributions, from fully dressed fermions and from their bosonic counterparts. It is interesting to note that the contributions of Cooper pairs and molecular bosons add in such a way that they form exactly one hybridized bosonic branch. The *local* entropy is thus given by a sum of fermionic and hybridized bosonic contributions:

$$\begin{aligned} S &= S_f + S_b \\ S_f &= -2 \sum_{\mathbf{k}} [f_k \ln f_k + (1 - f_k) \ln(1 - f_k)], \\ S_b &= - \sum_{q \neq 0} [b_q \ln b_q - (1 + b_q) \ln(1 + b_q)], \end{aligned} \tag{4}$$

where $f_k \equiv f(E_{\mathbf{k}})$, and $b_q \equiv b(\Omega_{\mathbf{q}} - \mu_{boson})$; a relatively small contribution associated with the T dependence of $\Omega_{\mathbf{q}}$ is not shown for clarity. The fermion contribution coincides with the standard BCS result for noninteracting Bogoliubov quasiparticles. And the bosonic contribution is given by the expression for non-directly-interacting bosons with dispersion $\Omega_{\mathbf{q}}$. These bosons are not free, however; because of interactions with the fermions their propagator contains important self energy effects. It should be noted that, due to our approximated form for the fermion self-energy, $\Sigma(K) = -\Delta_k^2 G_0(-K)$, all finite momentum pairs are essentially treated as if they were in the condensate in calculating S_f . This simplification can be removed at the cost of greater complexity (16, 8) without substantially affecting the physics discussed here. Interestingly, the Cooper pair component is accommodated in S_b , which represents the hybridized bosonic contribution.

After including the trap potential and internal binding energy of the bosons, the local energy can be decomposed into fermionic (E_f) and bosonic (E_b) contributions and directly computed

as follows

$$\begin{aligned}
E &= \mu n(r) + E_f + E_b, \\
E_f &= \sum_K (i\omega_n + \epsilon_{\mathbf{k}} - \mu(r)) G(K) \\
&= \sum_{\mathbf{k}} [2E_{\mathbf{k}} f_k - (E_{\mathbf{k}} - \epsilon_{\mathbf{k}} + \mu(r))] + \Delta^2 \chi(0), \\
E_b &= \sum_q (\Omega_{\mathbf{q}} - \mu_{boson}) b_q,
\end{aligned} \tag{5}$$

where $\mu(r) = \mu - V(r)$, $\omega_n = (2n + 1)\pi T$ is the fermionic Matsubara frequency, and the pair susceptibility $\chi(0)$ is given by the second term of the left hand side of Eq. (1). One can also calculate the entropy from the energy, $S = \int_0^T \frac{dT}{T} \frac{dE}{dT}$. We have verified that this gives the same result as obtained from Eqs. (4).

We have seen that both fermions and non-condensed bosons contribute to thermodynamics. It is of interest to decompose their contributions to the total entropy and reveal their spatial distributions. We illustrate this decomposition in Fig. S2 for the unitary case ($(k_F a)^{-1} = 0.11$) with $T = T_c/4$. To make contact with experiment (17) here we consider a realistic Gaussian trap potential, $V(r) = V_0[1 - e^{-m\omega^2 r^2/2V_0}]$, with trap depth $V_0/E_F = 14.6$ from experiment. It can be seen that the fermionic contribution (red curve) is limited to the trap edge as expected, since this is where the fermionic excitation gap is small. By contrast the bosonic contribution (green curve) is evenly distributed over the trap for all radii at which there is a condensate. This contribution rapidly decays at larger distances. Since the fermionic contribution depends on the magnitude of the gap and temperature, S_f has a different low T power law exponent at different $(k_F a)^{-1}$.

We next turn to the question of how to relate the theoretical and experimental temperature scales. To do this, in a collaboration with the authors of Ref. (17), we subjected the theoretically derived density profiles (6) to the same Thomas-Fermi (TF) fitting procedure as was used in experiment. Here two of the three dimensions of the spherical trap (18) were integrated

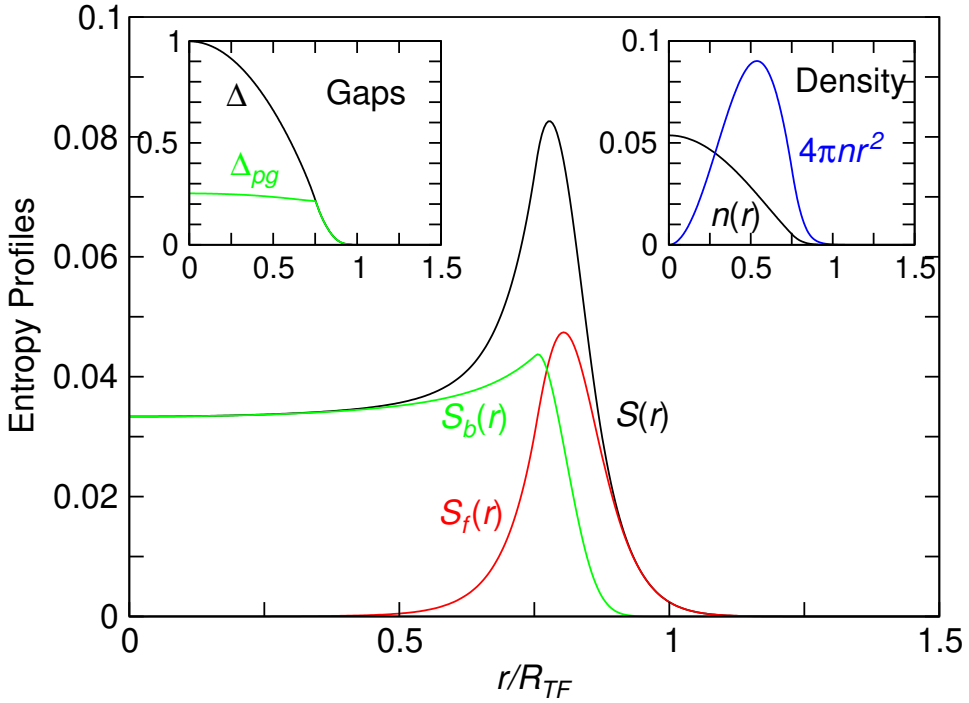


Figure S2: Decomposition of total entropy S (black curve) into fermionic (S_f , red) and bosonic (S_b , green) contributions, for the unitary case and Gaussian trap potential. The insets plot the excitation gaps $\Delta(r)$ (black) and pseudogap energy $\Delta_{pg}(r)$ (green) in units of noninteracting Fermi energy E_F , and density distributions $n(r)$ in units of k_F^3 . Here R_{TF} is the Thomas-Fermi radius. The insets share the same horizontal axis as the main figure.

over to obtain a one dimensional representation of the density profile. Our results are shown in Fig. S3. Quite remarkably, the TF-profile-deduced temperatures exactly coincided with the physical temperature above T_c . However, below T_c there was a systematic deviation so that the fitted profiles appeared to be at lower temperatures than they actually were. This is a consequence of condensate effects which lead to (albeit rather small) deviations from TF fits below T_c . This effect was compensated for in plotting the experimental data in Figs. 2 and 3 using the calibration curve shown here. Without this compensation, agreement between theory and experiment for Fig. 3 in the text is reasonable, but not as quantitatively precise.

Finally, in Fig. S4 we present a log-log plot comparing theory and experiment in the same fashion as in Ref. (17). This way of plotting the data also provides a more direct means of

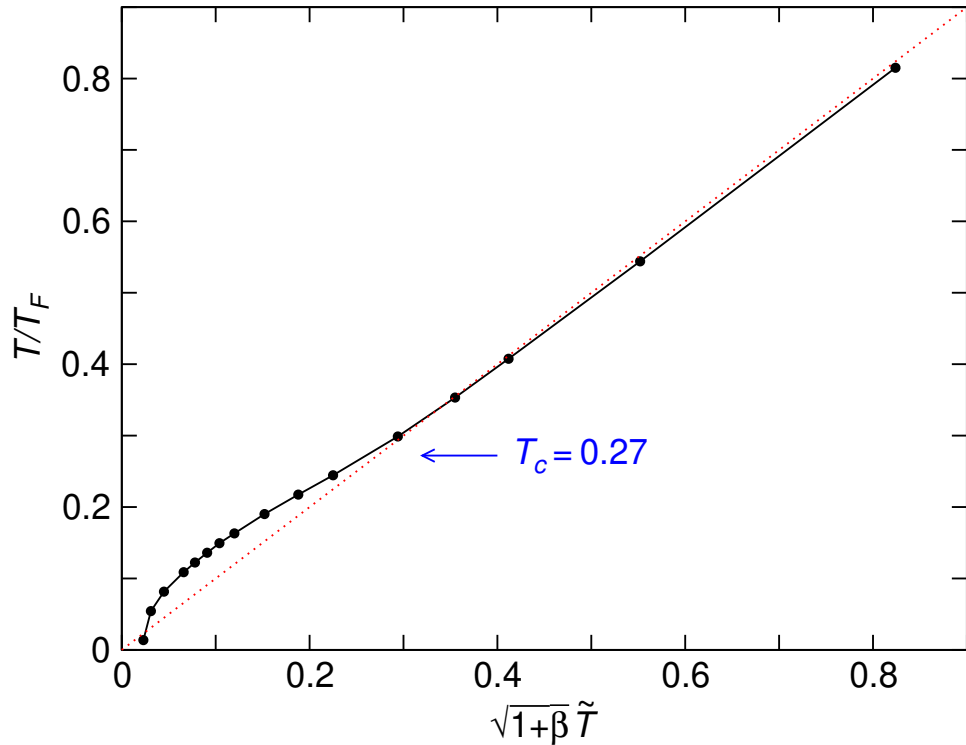


Figure S3: Temperature calibration: Theory versus experiment. T/T_F is the theoretical input, where T_F is the Fermi temperature. \tilde{T} and β are obtained using the fitting procedure in Ref. (17), and \tilde{T} is the experimental temperature parameter from the T-F fits. The red dotted line is the diagonal.

locating T_c as the temperature where the slope changes. Note that the slope change is quite smooth, consistent with the presence of a pseudogap.

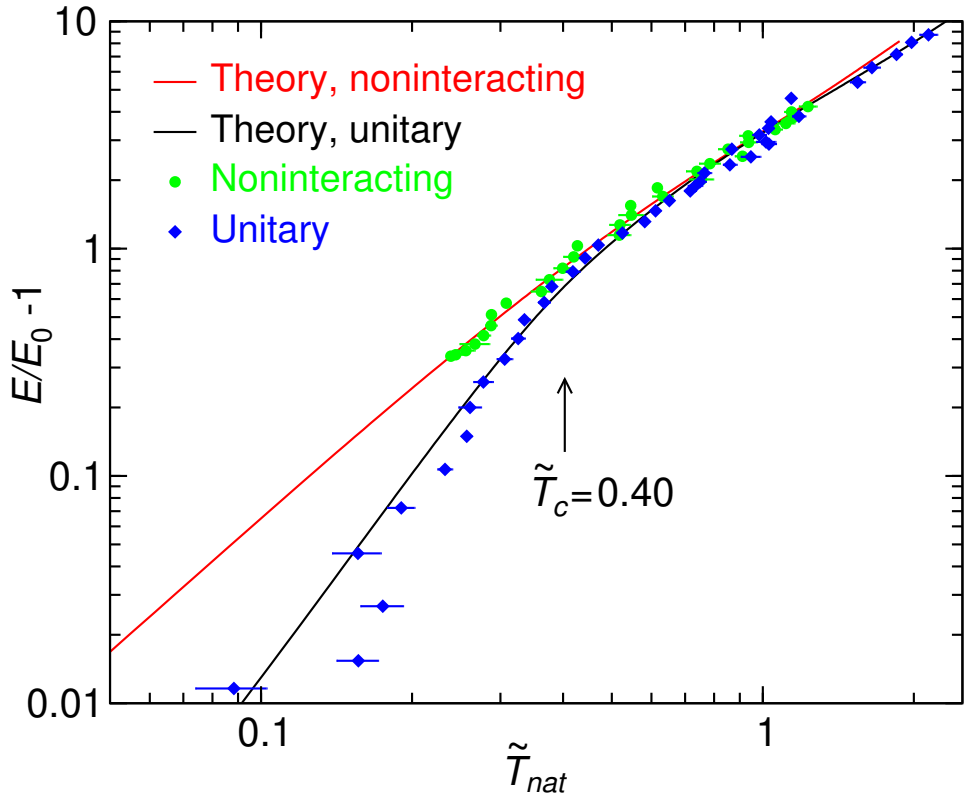


Figure S4: Comparison of present theory (lines) and experiments (symbols) of Ref. (17) in terms of $E/E_0 - 1$ as a function of $\tilde{T}_{nat} \equiv T/(T_F \sqrt{1 + \beta})$ on a log-log scale, for both unitary and non-interacting cases, with Gaussian trap potential having trap depth $V_0/E_F = 14.6$ as in experiment. The unitary data have been obtained from \tilde{T} by proper recalibration. The superfluid transition for the unitary case is manifested as a slope change across T_c . Here $E_0 \equiv E(T = 0)$, and $E_F = k_B T_F$ is the noninteracting Fermi energy.

References and Notes

1. A. J. Leggett, *Modern Trends in the Theory of Condensed Matter* (Springer-Verlag, Berlin, 1980), pp. 13–27.
2. A. Perali, P. Pieri, L. Pisani, G. C. Strinati, *Phys. Rev. Lett.* **92**, 220404 (2004).
3. A. Perali, P. Pieri, G. C. Strinati, *Phys. Rev. Lett.* **93**, 100404 (2004).
4. J. Stajic, *et al.*, *Phys. Rev. A* **69**, 063610 (2004).
5. J. Stajic, Q. J. Chen, K. Levin, Particle density distributions in fermi gas superfluids: Differences between one and two channel models in the BEC limit. Preprint available at <http://arXiv.org/abs/cond-mat/0402383>.
6. J. Stajic, Q. J. Chen, K. Levin, Measuring condensates in fermionic superfluids via density profiles in traps. Preprint available at <http://arXiv.org/abs/cond-mat/0408104>.
7. J. Kinnunen, M. Rodriguez, P. Törmä, *Science* **305**, 1131 (2004).
8. J. Maly, B. Jankó, K. Levin, *Physica C* **321**, 113 (1999).
9. Y. Ohashi, A. Griffin, *Phys. Rev. Lett.* **89**, 130402 (2002).
10. J. N. Milstein, S. J. J. M. F. Kokkelmans, M. J. Holland, *Phys. Rev. A* **66**, 043604 (2002).
11. Q. J. Chen, J. Stajic, S. N. Tan, K. Levin, BCS-BEC crossover: From high temperature superconductors to ultracold superfluids. Preprint available at <http://arXiv.org/abs/cond-mat/0404274>.
12. Outside the superfluid region in the trap, there are small but unimportant differences between μ_{pair} and μ_{boson} .

13. For a Gaussian trap, the relationship between E_F and N is slightly more complicated, but can be easily computed numerically by considering the noninteracting limit at $T = 0$, where $\mu = E_F$.
14. J. E. Williams, N. Nygaard, C. W. Clark, Phase diagrams for an ideal gas mixture of fermionic atoms and bosonic molecules. Preprint available at <http://arXiv.org/abs/cond-mat/0406617>.
15. Q. J. Chen, I. Kosztin, K. Levin, *Phys. Rev. Lett.* **85**, 2801 (2000).
16. Q. J. Chen, K. Levin, I. Kosztin, *Phys. Rev. B* **63**, 184519 (2001).
17. J. Kinast, A. Turlapov, J. E. Thomas, Heat capacity of a strongly interacting fermi gas. Preprint available at <http://arXiv.org/abs/cond-mat/0409283>.
18. It can be shown that trap anisotropy is not relevant for thermodynamical quantities because they involve integrals over the entire trap. The calculations can be mapped onto an equivalent isotropic system.